

# Divergence by Depth in an Oceanic Fish

Despite the striking physical and environmental gradients associated with depth variation in the oceans, relatively little is known about their impact on population diversification, adaptation and speciation. Changes in light associated with increasing depth are likely to alter the visual environment of organisms, and adaptive changes in visual systems may be expected. The pelagic beaked redbfish, *Sebastes mentella*, exhibits depth-associated patterns of substructure in the central North Atlantic, with a widely distributed shallow-pelagic population inhabiting waters between 250 and 550m depth and a deep-pelagic population dwelling between 550 and 800m. Here we performed a molecular genetic investigation of samples from fish collected from 'shallow' and 'deep' populations, using the mitochondrial control region and the gene coding for the visual-pigment rhodopsin. We identify patterns suggestive of potential adaptation to different depths, by detecting a specific amino acid replacement at the rhodopsin gene. Mitochondrial DNA results reflect a scenario of long-term demographic independence between the two *S. mentella* groups, and raise the possibility that these 'stocks' may in fact be two incipient species.

# 1 Divergence by Depth in an Oceanic Fish

2 Peter Shum<sup>1</sup>, Christophe Pampoulie<sup>2</sup>, Carlotta Sacchi<sup>3</sup>, and Stefano Mariani<sup>1\*</sup>

3 <sup>1</sup>School of Environment & Life Sciences, University of Salford, Manchester, UK

4 <sup>2</sup>Marine Research Institute, Reykjavík, Iceland

5 <sup>3</sup>School of Biology & Environmental Science, University College Dublin, Dublin, Ireland

6 \*Corresponding Author: [s.mariani@salford.ac.uk](mailto:s.mariani@salford.ac.uk)

## 7 Introduction

8 Speciation phenomena in taxa diverging with gene flow, in the absence of obvious geographic  
 9 barriers, remain a central focus in evolutionary biology (Bird et al., 2012; Smadja & Butlin, 2011;  
 10 Fitzpatrick, Fordyce & Gavrillets, 2008). The classical model of allopatric speciation involves the  
 11 evolution of reproductive isolation as a result of physical barriers that block gene flow in spatially  
 12 separated populations; whereas populations diverging in sympatry lead to the formation of  
 13 species from a single panmictic population which must exhibit strong divergent selection in order  
 14 to overcome the homogenizing effects of gene flow (Gavrillets, 2003). Parapatric speciation  
 15 represents an intermediate scenario of species formation whereby partial yet restricted contact  
 16 zones exist between two populations with limited gene exchange (Gavrillets, 2003). Although  
 17 exhaustive frameworks exist to identify and interpret speciation dynamics (Rettelbach et al.,  
 18 2013; Bird et al., 2012; Smadja & Butlin, 2011), only recently has empirical attention been  
 19 directed to the role of depth gradients in aquatic (Vonlathen et al., 2009) and especially oceanic  
 20 biota (Roy, Hurlbut & Ruzzante, 2012; Bird et al., 2011; Brokovich et al., 2010; Hyde et al.,  
 21 2008).

The strong physical gradients across depth layers in the ocean pose strong selective pressures in aquatic organisms (Ingram, 2011; Somero, 1992), and one notable factor is the change in the light environment (Warrant & Locket, 2004), which affects vision. Visual sensitivity in marine vertebrates depends on the spectral tuning mechanism of the visual pigment (VP) (Yokoyama, 2000), which consists of an opsin protein (part of the largest family of G-protein-coupled receptors) bound to a light-sensitive chromophore. Differently-charged amino acid (AA) residues in the opsin will result in slightly different light absorbance by the photoreceptor cells (Yokoyama, 2002).

The percomorph marine family of rockfishes (Sebastidae) have played a central role in the understanding of depth-associated population divergence and speciation in the ocean (Ingram, 2011; Stefánsson et al., 2009a; Hyde et al., 2008; Alesandrini & Bernardi, 1999), and evidence exists that the rhodopsin gene may have evolved in response to different light environments in the main, ancient radiation of the genus, in the Pacific (Sivasundar & Palumbi, 2010). North-Atlantic *Sebastes* have a much more recent history (Hyde & Vetter, 2007), with the four recognised extant species having diversified during the Pleistocene (Bunke, Hanel, & Trautner, 2012). In particular, the beaked redfish, *Sebastes mentella*, consists of two genetically distinguishable groups (Stefánsson et al., 2009a; Pampoulie & Daniélsdóttir, 2008): a widely-distributed shallow-pelagic (SP) form, found between 250 and 550m depth and a more circumscribed deep-pelagic (DP) component, between 550 and 800m. However, doubts remain as to the forces at play and the time scales associated with this divergence (Stefánsson et al., 2009b; Cadrin et al., 2010).

Here, we sought to investigate whether on-going processes of adaptation to different depth layers may leave a signature of disruptive selection in the rhodopsin gene in a recently diversifying *Sebastes* species. We also employed for the first time the mitochondrial DNA control region to reconstruct historical demography and to further elucidate the evolutionary relationships between ‘shallow’ and ‘deep’ pelagic beaked redfish.

## Material and Methods

### Generation of molecular data

Archive samples were randomly selected from 25 shallow-pelagic (SP) (collected above 400m depth) and 25 deep-pelagic (DP) (collected below 700m) *Sebastes mentella* from the Irminger Sea, south-west of Iceland previously genotyped by Stéfansson et al. (2009b) (sample numbers 4&5 in the original article). DNA was isolated from gill tissue that had been preserved in 96% EtOH using a modified salt extraction protocol (Miller et al., 1988) or the DNeasy kit (Qiagen ©) following the manufacturer's protocol. The non-coding mitochondrial control region was amplified by PCR using primers developed by Hyde & Vetter (2007); D-RF: 5'-CCT GAA AAT AGG AAC CAA ATG CCA G-3' and Thr-RF: 5'-GAG GAY AAA GCA CTT GAA TGA GC-3'. The primers by Chen et al. (2003); Rh193: 5'-CNT ATG AAT AYC CTC AGT ACT ACC-3' and Rh1039r: 5'-TGC TTG TTC ATG CAG ATG TAG A-3' were used to amplify 744 bp of the intron-free rhodopsin gene in 10 shallow-pelagic *S. mentella*, 12 deep-pelagic *S. mentella*, and 3 and 4 individuals of *S. marinus* and *S. viviparus* as outgroups. Reactions were carried out in 25µl volumes containing 1x PCR buffer, 1 mM MgCl<sub>2</sub>, 200µM dNTPs, 0.4 µM of each primer, 0.2 units *Taq* DNA polymerase, with 1 µl of DNA template for mtDNA (4 µl for rhodopsin). Amplifications were performed in a Biometra T3000 Thermocycler using the following temperature profiles: control region: 94°C (2 min), 35 cycles of [94°C (30 sec), 59°C (60 sec), 72 °C (60 sec)], followed by 3 minutes at 72 °C; for rhodopsin: 95 °C (5 min), 37 cycles of [94 °C (20 sec), 58 °C (30 sec), 72 °C (45 sec)], followed by 5 minutes at 72 °C. A negative control was included in all reactions. PCR products were subjected to electrophoresis through a 1% agarose gel 1X Tris–Borate–EDTA Buffer, stained with SYBR green for visualisation via a UV-transilluminator and then purified through the addition of exonuclease I and shrimp alkaline phosphatase to remove unincorporated primers and deoxynucleotides in preparation to sequencing. Purified products were sequenced by Macrogen (Macrogen, Amsterdam, Europe; <http://dna.macrogen.com/eng/>).

### Data Analysis

#### Genetic diversity and population differentiation

The mtDNA control region was examined for nucleotide and haplotype diversity. This included the number of net nucleotide substitutions per site between populations ( $D_a$ ) which was calculated using DnaSP v5.10 (Librado & Rozas, 2009). We estimated the level of genetic variation between populations calculating pairwise population  $F_{ST}$

and  $\Phi_{st}$  values performed in ARLEQUIN v3.5.1.2 (Excoffier & Lischer, 2010) with significant values tested by 5000 permutations.

Mismatch analysis was performed to examine the demographic history between the shallow-pelagic and deep-pelagic *S. mentella* populations using ARLEQUIN and distributions were compared with a two-sample Kolmogorov-Smirnov (K-S) test. For populations at stationary demographic equilibrium, theoretical and empirical studies show that the mismatch distributions usually have multimodal, ragged or erratic distributions, and are typically smoother or unimodal for populations that have undergone a recent expansion (Rogers & Harpending, 1992). To test the goodness-of-fit distribution, we calculated the sum of squared deviations (SSD) and raggedness index (r) for a stepwise expansion model for the data tested by Monte Carlo Markov Chain simulations (1000 steps) in ARLEQUIN.

Haplotype genealogies for the *S. mentella* data set were constructed following a method described by Salzburger et al. (2011) based on a maximum likelihood tree for mtDNA and rhodopsin genes sequences.

Data from a selected suite of 12 microsatellite loci previously used for genotyping by Stéfansson et al. (2009b) were used to calculate pairwise genetic differentiation (Weir & Cockerham's  $F_{ST}$ , Hedricks  $G'_{ST}$  & Jost's  $D_{est}$ ) between populations with 9999 permutations carried out to obtain significance levels using GenAIEx 6.501 software (Peakall & Smouse, 2006). Population structure was visualized by correspondence analysis (CA) using GENETIX 4.05 (Belkhir et al. 1996).

#### *Phylogenetic analysis and test for positive selection*

Maximum-likelihood (ML) analyses of the rhodopsin gene sequences were performed using PhyML 3.0 (Guindon & Gascuel, 2003) under 1,000 replications; using Modeltest3.7 (Posada & Crandall, 1998), the model that best fit the data was found to be F81+I (pinvar=0.9770). Trees generated from these results were used for a test for positive selection at the rhodopsin gene, conducted using the Creevey-McInerney method (Creevey & McInerney, 2002) implemented in CRANN (Creevey & McInerney, 2003). This test is a more sensitive tree-based analysis derived from the relative ratio test (McDonald & Kreitmann, 1991). Given an appropriate rooted tree, the number of synonymous and non-synonymous substitutions are calculated along each internal branch using the reconstructed ancestral sequences. The method uses statistical tests for independence ( $\chi^2$  G-test or Fisher's exact test) to evaluate

whether the ratio between synonymous (Silent Invariable (SI) to Silent Variable (SV)) and non-synonymous (Replacement Invariable (RI) to Replacement Variable (RV)) substitutions deviate from the expected value under the neutral model. Where the G-test fails to produce a result, the Fisher's test is used and vice versa. Positive directional selection is expected if there is a significantly higher number of RI substitutions or non-directional selection if  $RV > RI$ . The test was performed using *S. alutus* as outgroup (Fig. 3) as it represents the closest common ancestor for the Atlantic *Sebastes* spp. (Hyde & Vetter, 2007).

## Results and Discussion

We recovered 16 mtDNA haplotypes, defined by 15 total variable sites across the two groups. Haplotypes were almost completely segregated between depth layers, with eight haplotypes found in the deep, never recovered in the shallow area, and resembling a starburst pattern, three mutational steps away from the rest of the network (Fig. 1a). Of the 10 haplotypes found in the shallow, eight were exclusive of this habitat, and only two individuals collected in the deep were found to bear a 'shallow-type' sequence. The shallow-pelagic (SP) group exhibited much greater diversity ( $\hat{h}=0.887\pm0.033$ ,  $\pi=0.00504\pm0.00082$ ) than the deep-pelagic (DP) group ( $\hat{h}=0.543\pm0.119$ ,  $\pi=0.00238\pm0.00071$ ) (Table 1).

Partitioning of genetic variance between the populations showed highly significant and strong population structure (Table. 2). The mismatch distributions of the two groups (Fig. 1b) were significantly different (K-S test:  $D_{300}=0.3$ ,  $p<<0.001$ ), and confirmed what is visually apparent from the haplotype network: a scenario of more recent and pronounced demographic and spatial expansion in the deep-pelagic group compared to the shallow-pelagic (Table 3). Using Nei's (Nei, 1987) formula for divergence time:  $T=D_a/2\mu$ , where  $2\mu$  represents a general mtDNA evolutionary rate, commonly assumed to be around 11% per million years for fish mtDNA control region

(Patarnello, Volckaert & Castilho, 2007), we find that the “deep” and “shallow” lineages split over 44,000 years ago.

The rhodopsin gene was tested for signatures of positive selection using the Creevey-McInerney method rooting the tree with *S. alutus* as an outgroup (Fig. 2). Values for the four substitution variables, G-test, and *p*-values along each branch are presented in Table 4. Two branches (numbers 26 and 27) showed significance at the *p*=0.05 level (Fig. 2). Branches 26 and 27 show significant RI to RV deviations from neutrality, due to non-synonymous substitutions (Table 3), suggesting that positive disruptive selection is acting on the rhodopsin gene for the clade and on the internal branch leading to the shallow group. We observed a fixed non-synonymous AA substitution within the transmembrane domain, which strongly discriminates the two groups inhabiting shallow and deep environments (Fig. 3). The shallow-pelagic group exhibits a GTC at position 119, which codes for Valine (L119V), while the deep-pelagic type displays an ATC, coding for Isoleucine (L119I). Amino acid changes located in the transmembrane helical regions have been known to be important for spectral tuning (Yokoyama et al., 2008), yet *in-vitro* experimental spectral analyses of vertebrate rhodopsins suggest that amino acid substitutions at site 119 have negligible effect on absorption spectra (Yokoyama et al., 2008). Nevertheless, substitutions within the transmembrane protein domain III (helix-III), such as site 119, have been shown to affect the decay rate of metarhodopsin II (“meta II”; Ou et al., 2011), which is an intermediate of rhodopsin that binds and activates transducin, the visual G-protein (Smith, 2010). Ou et al. (2011) have shown that an AA replacement L119C against the wild-type rhodopsin resulted in shorter meta II lifetimes, suggesting more responsive structural alterations at the helix’ G-protein binding site.

Neither spectral nor conformational analyses have so far been conducted on shallow-pelagic and deep-pelagic *Sebastes mentella*, but the AA variation observed here could underlie differential

hydrophobic activity and photoisomerization sensitivity (Ou et al., 2011) that could hold some adaptive value, even without net change in wavelength of maximal absorption.

Sivasundar and Palumbi (2010) discovered a striking association between AA replacements along the rhodopsin gene and inferred depth preference in many North Pacific *Sebastes*. Interestingly, four North-Pacific *Sebastes* (*S. chlorostictus*, *S. elongates*, *S. aurora* and *S. melanostomus*) typically associated with deeper waters were observed to exhibit the same AA replacement L119I as detected in the deep-sea *S. mentella*. Similarly, one Pacific species (*S. diploproa*) exhibits the AA replacement L119V, which is linked to a shift back to shallower waters, and mirrors the polymorphism in the shallow-pelagic *S. mentella*.

Although larger sample sizes will be required in the future to test these patterns more robustly, the implications of these findings are twofold, and have powerful resonance for both marine evolution and fisheries management. First, mitochondrial variation between ‘shallow’ and ‘deep’ *S. mentella* in the North Atlantic unveil a degree of historical divergence that previously employed genetic markers either failed to detect (Bunke et al., 2012) or could not reliably frame in a phylogeographic context (Stefánsson et al., 2009b).

The level of differentiation and haplotype sorting is such that evolutionary independence can be broadly upheld for these two habitat-segregated lineages, and re-analysis of microsatellite data confirm this picture (Fig. 4). In particular, the comparison of frequency-based indicators of substructure ( $F_{ST}$  for mtDNA, and  $G'_{ST}$  and  $D_{est}$  to account for the hypervariability of microsatellite loci) reveal values (Table 2) that match theoretical expectations under neutral divergence, taking into account the four-fold strength of genetic drift at mitochondrial markers. Interestingly, we also noticed two individuals with a ‘shallow-type’ mtDNA haplotype, which were caught in the deep layer. One of these two (DP29, Fig. 2) also screened at the rhodopsin locus, exhibits a sequence typical of the shallow layer, and its multilocus microsatellite genotype



also falls with the shallow group (Fig. 4), which can be interpreted as the occurrence of individual movements along the water column during the life cycle (i.e. short-term “dives” into the deep, by shallow-dwelling fish). Another deep-caught individual (DP1) also exhibits a “shallow” haplotype, but a “deep-like” ATC rhodopsin sequence and an inconclusive multilocus microsatellite genotype (Fig. 4). Collectively, this likely reflects the occurrence of introgressive hybridisation between the two groups, as previously suggested by Pampoulie & Danielsdottir (2008).

Furthermore, the stark pattern of depth-associated divergence at the rhodopsin gene is perhaps even more surprising, were it not for the fact that comparable evolutionary genetic patterns have recently been credited with a key role in the diversification of the more ancient Pacific *Sebastes* group (Sivasundar & Palumbi, 2010). It has been hypothesized that fast-evolving markers will allow to determine recent speciation events for closely related *Sebastes* spp. (Alesandrini & Bernardi, 1999; Cadrin et al., 2010). The present data provide a snapshot of the evolutionary mechanisms that may be at play in the young, species-poor, Atlantic *Sebastes* lineage, during its initial phase of adaptive radiation, underpinned by positive selection at the rhodopsin gene.

Less than a decade ago, *S. mentella* was assumed to be panmictic in the North Atlantic, and the rapidly increasing fishery pressure on these stocks did not recognise any possible substructure until 2009 (Cadrin et al., 2010). These latest results dismiss the notion of panmixia in this oceanic species, and, perhaps more intriguingly, open the possibility that the two ‘shallow’ and ‘deep’ groups may represent two lineages experiencing adaptation towards divergent environmental conditions. In the near future, it should be experimentally evaluated whether the amino acid replacements at the 119 position actually produce detectable changes in retinal absorbance or structural responsiveness, and whether more powerful molecular comparisons covering a wider

193 portion of the genome (e.g. SNP-based genome scans; transcriptomic approaches) will offer  
 194 further insights into the role of depth as a diversifying agent in the ocean.

## 195 **Acknowledgements**

196 We are grateful to the WKREDS workshop of the International Council for the Exploration of the  
 197 Sea (ICES) for inspiring this work. We are also indebted to Valerie Chosson for technical  
 198 assistance at the MRI, and Emma Teeling, Bruno Fonseca Simões and three reviewers, for the  
 199 constructive criticism offered.

## References

- Alesandrini S, Bernardi G. 1999. Ancient species flocks and recent speciation events: what can rockfish teach us about cichlids (and vice versa)? *Journal of Molecular Evolution* 49:814–818.
- Belkhir K, Borsa P, Chikhi L, Raufaste N, & Bonhomme F. 1996. GENETIX 4.05, logiciel sous Windows TM pour la génétique des populations. Laboratoire Génome, Populations, Interactions, CNRS UMR 5000, Université de Montpellier II, Montpellier (France).
- Bird CE, Fernandez-Silva I, Skillings DJ, Toonen RJ. (2012) Sympatric speciation in the post “modern synthesis” era of evolutionary biology. *Evolutionary Biology* 39: 158–180.
- Bird CE, Holland BS, Bowen BW, Toonen RJ. 2011. Diversification of sympatric broadcast-spawning limpets (*Cellana* spp.) within the Hawaiian archipelago. *Molecular Ecology* 20: 2128–2141.
- Brokovich E, Ben-Ari T, Kark S, Kiflawi M, Dishon G, Iluz D, Shashar N. 2010. Functional changes of the visual system of the damselfish *Dascyllus marginatus* along its bathymetric range. *Physiology and Behavior* 101: 413–421.
- Bunke C, Hanel R, Trautner JH. 2012. Phylogenetic relationships among North Atlantic redfish (genus *Sebastes*) as revealed by mitochondrial DNA sequence analysis. *Journal of Applied Ichthyology* 29:82-92.
- Cadrin SX, Bernreuther M, Daniélsdóttir AK, Hjörleifsson E, Johansen T, Kerr L, Kristinsson K, Mariani S, Nedreaas K, Pampoulie C, Planque B, Reinert J, Saborido-Rey F, Sigurðsson T, Stransky C. 2010. A Population structure of beaked redfish, *Sebastes mentella*: evidence of divergence associated with different habitats. *ICES Journal of Marine Science* 67:1617–1630.
- Chen W-J, Bonillo C, Lecointre G. 2003. Repeatability of clades as a criterion of reliability: a case study for molecular phylogeny of Acanthomorpha (Teleostei) with larger number of taxa. *Molecular Phylogenetics and Evolution* 26: 262-288.

- 226 Creevey CJ, McInerney JO. 2002. An algorithm for detecting directional and non-directional  
227 positive selection, neutrality and negative selection in protein coding DNA sequences. *Gene*  
228 300:43-51.
- 229 Creevey CJ, McInerney JO. 2003. CRANN: detecting adaptive evolution in. *Bioinformatics*  
230 19:1726.
- 231 Excoffier L, Lischer HE. 2010. Arlequin suite ver 3.5: a new series of programs to perform  
232 population genetics analyses under Linux and Windows. *Molecular Ecology Resources* 10:  
233 564–567.
- 234 Fitzpatrick BM, Fordyce JA, Gavrilets S. 2008. What, if anything, is sympatric speciation?  
235 *Journal of Evolutionary Biology* 21:1452–1459.
- 236 Gavrilets S. 2003. Perspective: models of speciation: what have we learned in 40 years?  
237 *Evolution* 57:2197-2215.
- 238 Guindon S, Dufayard JF, Anisimova M., Hordijk W, Gascuel O. 2010. PhyML 3.0: new algorithms,  
239 methods and utilities. *Systematic Biology* 59:307-321.
- 240 Hyde JR, Kimbrell CA, Budrick JE, Lynn EA, Vetter RD. 2008. Cryptic speciation in the  
241 vermilion rockfish (*Sebastes miniatus*) and the role of bathymetry in the speciation process.  
242 *Molecular Ecology* 17:1122-1136.
- 243 Hyde J, Vetter RD. 2007. The origin, evolution, and diversification of rockfishes of the genus  
244 *Sebastes* (Cuvier). *Molecular phylogenetics and evolution* 44:790-811.
- 245 Ingram T. 2011. Speciation along a depth gradient in a marine adaptive radiation. *Proceedings of*  
246 *the Royal Society of London Series B* 278: 613–618.

- 247 Librado P, Rozas J. 2009. DnaSP v5: a software for comprehensive analysis of DNA  
248 polymorphism data. *Bioinformatics* 25: 1451-1452.
- 249 McDonald JH, & Kreitman M. 1991. Adaptive protein evolution at the Adh locus in Drosophila.  
250 Nature 351: 652-654.
- 251 Miller SA, Dykes DD, & Polesky H F. 1988. A simple salting out procedure for extracting DNA  
252 from human nucleated cells. *Nucleic Acids Research* 16: 1215.
- 253 Nei M. 1987. *Molecular Evolutionary Genetics*. Columbia University Press, New York, NY.
- 254 Ou WB, Yi T, Kim JM, Khorana HG. 2011. The roles of transmembrane domain Helix-III during  
255 rhodopsin photoactivation. *PLoS One* 6:e17398.
- 256 Pampoulie C. Daniélsdóttir AK. 2008. Resolving species identification problems in the genus  
257 *Sebastes* using nuclear genetic markers. *Fisheries Research* 93:54-63.
- 258 Patarnello T, Volckaert F. Castilho R. 2007. Pillars of hercules: Is the atlantic-mediterranean  
259 transition a phylogeographical break? *Molecular Ecology* 16:4426-4444.
- 260 Peakall R, Smouse PE. 2006. Genalex 6: genetic analysis in Excel. Population genetic software  
261 for teaching and research. *Molecular Ecology Notes* 6: 288-295.
- 262 Posada D, Crandall KA. 1998. MODELTEST: testing the model of DNA substitution.  
263 *Bioinformatics* 14:817-818.
- 264 Rettelbach A, Kopp M, Dieckmann U, & Hermisson J. 2013. Three Modes of Adaptive  
265 Speciation in Spatially Structured Populations. *The American Naturalist* 182: E215-E234.
- 266 Rogers AR, & Harpending H. 1992. Population growth makes waves in the distribution of  
267 pairwise genetic differences. *Molecular Biology and Evolution* 9: 552-569.

- 268 Roy D, Hurlbut TR, Ruzzante DE. 2012. Biocomplexity in a demersal exploited fish, white hake  
269 (*Urophycis tenuis*): depth-related structure and inadequacy of current management  
270 approaches. *Canadian Journal of Fisheries and Aquatic Sciences* 69:415-429.
- 271 Salzburger W, Ewing GB, von Haeseler A. 2011. The performance of phylogenetic algorithms in  
272 estimating haplotype genealogies with migration. *Molecular Ecology* 20:1952-1963.
- 273 Sivasundar A, Palumbi SR. 2010. Parallel amino acid replacements in the rhodopsins of the  
274 rockfishes (*Sebastes* spp.) associated with shifts in habitat depth. *Journal of Evolutionary*  
275 *Biology* 23:1159-1169.
- 276 Smadja CM, & Butlin RK. 2011. A framework for comparing processes of speciation in the  
277 presence of gene flow. *Molecular Ecology* 20:5123-5140.
- 278 Smith SO. 2010. Structure and activation of the visual pigment rhodopsin. *Annual Review of*  
279 *Biophysics* 39:309-328.
- 280 Somero G N. 1992. Adaptations to high hydrostatic pressure, *Annual review of physiology*  
281 54:557-577.
- 282 Stefánsson MO, Reinert J, Sigurðsson Þ, Kristinsson K, Nedreaas K, Pampoulie C. 2009a. Depth  
283 as a potential driver of genetic structure of *Sebastes*. *ICES Journal of Marine Science*  
284 66:680-690.
- 285 Stefánsson MÖ, Sigurðsson T, Pampoulie C, Daniëlsdóttir AK, Thorgilsson B, Ragnarsdóttir R,  
286 Gíslason D, Coughlan J, Cross TF, Bernatchez L. 2009b. Pleistocene genetic legacy suggests  
287 incipient species of *Sebastes mentella* in the Irminger Sea. *Heredity* 102:514-524.

- 288 Vonlanthen P, Roy D, Hudson AG, Largiader CR, Bittner D, Seehausen O. 2009. Divergence  
289 along a steep ecological gradient in lake whitefish (*Coregonus* sp.). *Journal of Evolutionary*  
290 *Biology* 22:498–514.
- 291 Warrant EJ, Locket N. 2004. Vision in the deep sea. *Biological Reviews* 79:671-712.
- 292 Yokoyama S. 2000. Molecular evolution of vertebrate visual pigments. *Progress in Retinal and*  
293 *Eye Research* 19:385-419.
- 294 Yokoyama S. 2002. Molecular evolution of color vision in vertebrates. *Gene* 300:69-78.
- 295 Yokoyama S, Tada T, Zhang H, Britt L. 2008. Elucidation of phenotypic adaptations: Molecular  
296 analyses of dim-light vision proteins in vertebrates. *Proceedings of the National Academy of*  
297 *science of the United State of America* 105:13480–13485.

**Table 1.** Summary of mtDNA control region molecular

diversity: H = unique haplotypes; n = number of individuals; S

| Population | H/n  | S  | $\hat{h} \pm \text{SD}$ | $\pi \pm \text{SD}$ | $D_T$    | $F_S$  | $F^*$    | $D^*$    |
|------------|------|----|-------------------------|---------------------|----------|--------|----------|----------|
| (SP)       | 8/25 | 10 | 0.887±0.033             | 0.00504±0.00082     | -1.08590 | -3.806 | -2.30037 | -2.35314 |
| (DP)       | 6/25 | 8  | 0.543±0.119             | 0.00238±0.00071     | -1.77639 | -4.717 | -1.49744 | -1.08199 |

= Segregating sites;  $\hat{h}$  = haplotype diversity;  $\pi$  = nucleotide

diversity (both with associated standard deviations, SD);  $D_T$  =

Tajima's  $D$ ;  $F_S$  = Fu's  $F_S$  statistic;  $F^*$  = Fu and Li's  $F$  test;  $D^*$  =

Fu and Li's  $D$  test. SP = Shallow Pelagic; DP = Deep Pelagic.

**Table 2.** Analysis of fixation/differentiation indices for mtDNA and microsatellite data between shallow-pelagic (SP) and deep-pelagic (DP) *S. mentella*.

| Marker          | Group    | Fixation/Differentiation index | estimate | $p$    |
|-----------------|----------|--------------------------------|----------|--------|
| mtDNA           | SP vs DP | $F_{ST}$                       | 0.636    | <0.001 |
|                 |          | $\Phi_{ST}$                    | 0.273    | <0.001 |
| Microsatellites | SP vs DP | $F_{ST}$                       | 0.031    | 0.001  |
|                 |          | $G'_{ST}$                      | 0.135    | 0.001  |
|                 |          | $D_{est}$                      | 0.121    | 0.001  |



306 **Table 3.** Mismatch distribution parameter estimates for mtDNA control region

| Population | Mismatch Distribution |            |            |   |                                    |
|------------|-----------------------|------------|------------|---|------------------------------------|
|            | $\tau$                | $\theta_0$ | $\theta_1$ | SSD $p$ -value $\pm$ SD                     | r $p$ -value $\pm$ SD              |
| (SP)       | 1.9                   | 0.0000     | 99,999     | DE 0.007 $\pm$ 0.18<br>SE 0.007 $\pm$ 0.002 | 0.30 $\pm$ 0.21<br>0.27 $\pm$ 0.28 |
| (DP)       | 0.1                   | 0.0000     | 99,999     | DE 0.274 $\pm$ 0.18<br>SE 0.004 $\pm$ 0.002 | 0.00 $\pm$ 0.21<br>0.67 $\pm$ 0.28 |

$\tau$  = tau;  $\theta_0$  = theta 0;

307  $\theta_1$  = theta 1; SSD = sum of squared deviations; r = raggedness

308 statistic; DE: demographic expansion, SE: spatial expansion; (SP) = Shallow pelagic; (DP) = Deep-

309 pelagic.

311 **Table 4.** Creevey-McInerney positive selection analysis on *Sebastes* rhodopsin sequences  
 312 outgrouped with *S. alutus* (GenBank: EF212407.1), G-value p<0.05 for Fisher's<sup>†</sup> and G-Test\*

| Branch no.       | RI | RV | SI | SV | G-value          |
|------------------|----|----|----|----|------------------|
| <b>rhodopsin</b> |    |    |    |    |                  |
| 0                | 0  | 2  | 0  | 0  | 0.00             |
| 1                | 0  | 2  | 0  | 0  | 0.00             |
| 2                | 0  | 2  | 0  | 0  | 0.00             |
| 3                | 0  | 5  | 0  | 0  | 0.00             |
| 4                | 0  | 5  | 0  | 0  | 0.00             |
| 5                | 0  | 5  | 0  | 0  | 0.00             |
| 6                | 0  | 5  | 0  | 0  | 0.00             |
| 7                | 0  | 5  | 0  | 0  | 0.00             |
| 8                | 0  | 5  | 0  | 0  | 0.00             |
| 9                | 0  | 5  | 0  | 0  | 0.00             |
| 10               | 0  | 5  | 0  | 0  | 0.00             |
| 11               | 0  | 8  | 0  | 0  | 0.00             |
| 12               | 0  | 8  | 0  | 0  | 0.00             |
| 13               | 0  | 8  | 0  | 0  | 0.00             |
| 14               | 0  | 8  | 0  | 0  | 0.00             |
| 15               | 0  | 8  | 0  | 0  | 0.00             |
| 16               | 0  | 11 | 1  | 0  | 2.01             |
| 17               | 0  | 0  | 1  | 0  | 0.00             |
| 18               | 0  | 9  | 0  | 0  | 0.00             |
| 19               | 0  | 11 | 0  | 0  | 0.00             |
| 20               | 0  | 12 | 0  | 0  | 0.00             |
| 21               | 0  | 12 | 0  | 0  | 2.2              |
| 22               | 0  | 12 | 1  | 0  | 2.2              |
| 23               | 0  | 12 | 1  | 0  | 2.2              |
| 24               | 0  | 12 | 1  | 0  | 2.2              |
| 25               | 0  | 12 | 1  | 0  | 2.2              |
| 26               | 1  | 12 | 2  | 0  | 5.5 <sup>†</sup> |
| 27               | 8  | 24 | 5  | 1  | 6.76*            |

# 313 FIGURE CAPTIONS

314 **Figure 1.** *Sebastes mentella* genealogies for mtDNA (n=50; 25 SP + 25 DP) and rhodopsin  
315 (n=22; 10 SP + 12 DP), and mtDNA mismatch distributions. (A) Haplotype network for the  
316 shallow (red) and deep (blue) groups for mtDNA (i) and rhodopsin (ii). The size of each circle  
317 represents the proportion of haplotypes. The lengths of the connecting lines reflect the number of  
318 mutations between haplotypes. (B) Mismatch distributions from the mtDNA sequences of  
319 shallow (i) and deep (ii) groups, respectively from above and below 550 metres depth  
320 respectively. Dotted lines (Up/low bound.) represent the 95% boundaries of the simulated  
321 distributions.

322 **Figure 2.** Creevey–McInerney analysis of *Sebastes* rhodopsin. Rhodopsin reveals significant  
323 positive selection (\*) at two nodes (26, 27).

324 **Figure 3.** Chromatograms illustrating the non-synonymous A/G mutation on the rhodopsin gene,  
325 which discriminates between “Deep-Pelagic” (a: above) and “Shallow-Pelagic” (b: below)  
326 *Sebastes mentella*.

327 **Figure 4.** Correspondence analysis based on microsatellite data. Each circle represent an  
328 individual, red and blue refer to the shallow-pelagic (SP) and deep-pelagic (DP) groups  
329 respectively.

# Figure 1

Comprehensive image of mtDNA and Rhodopsin genetic divergence and Mismatch Distributions

Figure 1. *S. mentella* genealogies for mtDNA (n=50; 25 SP + 25 DP) and rhodopsin (n=22; 10 SP + 12 DP), and mtDNA mismatch distributions. (A) Haplotype network for the shallow (red) and deep (blue) groups for mtDNA (i) and rhodopsin (ii). The size of each circle represents the proportion of haplotypes. The lengths of the connecting lines reflect the number of mutations between haplotypes. (B) Mismatch distributions from the mtDNA sequences of shallow (i) and deep (ii) groups, respectively from above and below 550 metres depth respectively. Dotted lines (Up/low bound.) represent the 95% boundaries of the simulated distributions.

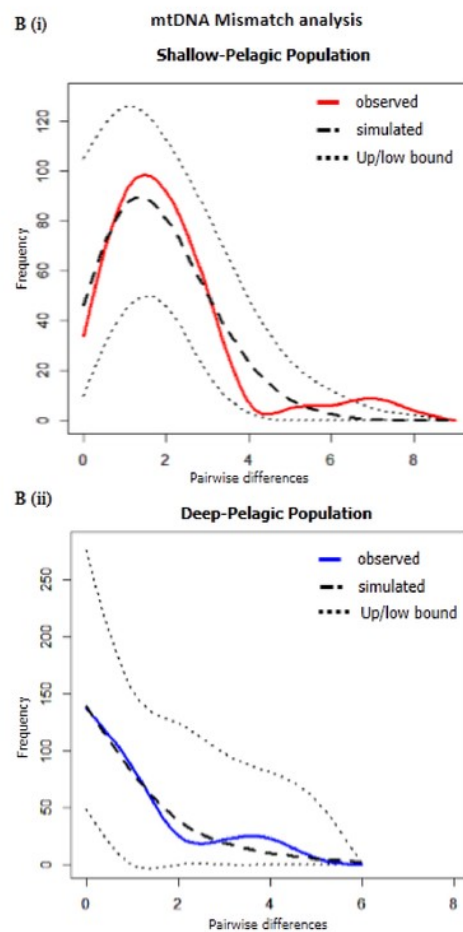
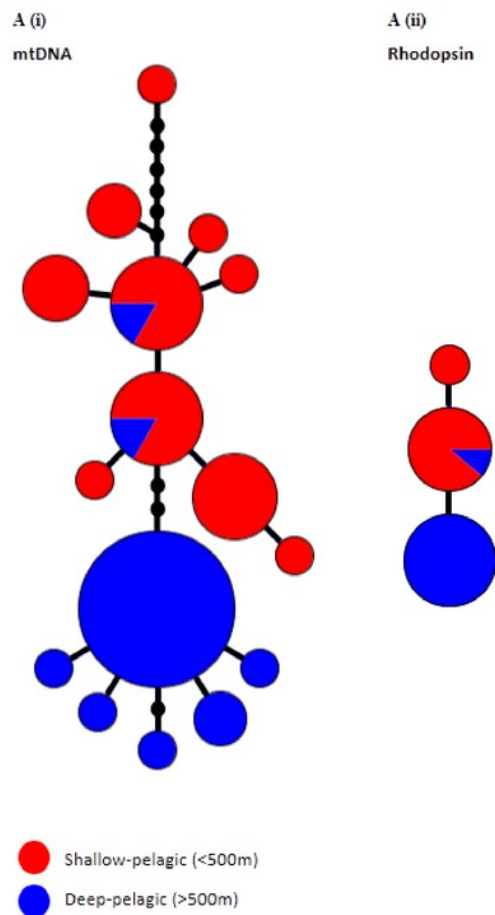


## Figure 2

### CRANN test tree

Creevey–McInerney analysis of *Sebastes* rhodopsin. Rhodopsin reveals significant positive selection (\*) at two nodes (26, 27).

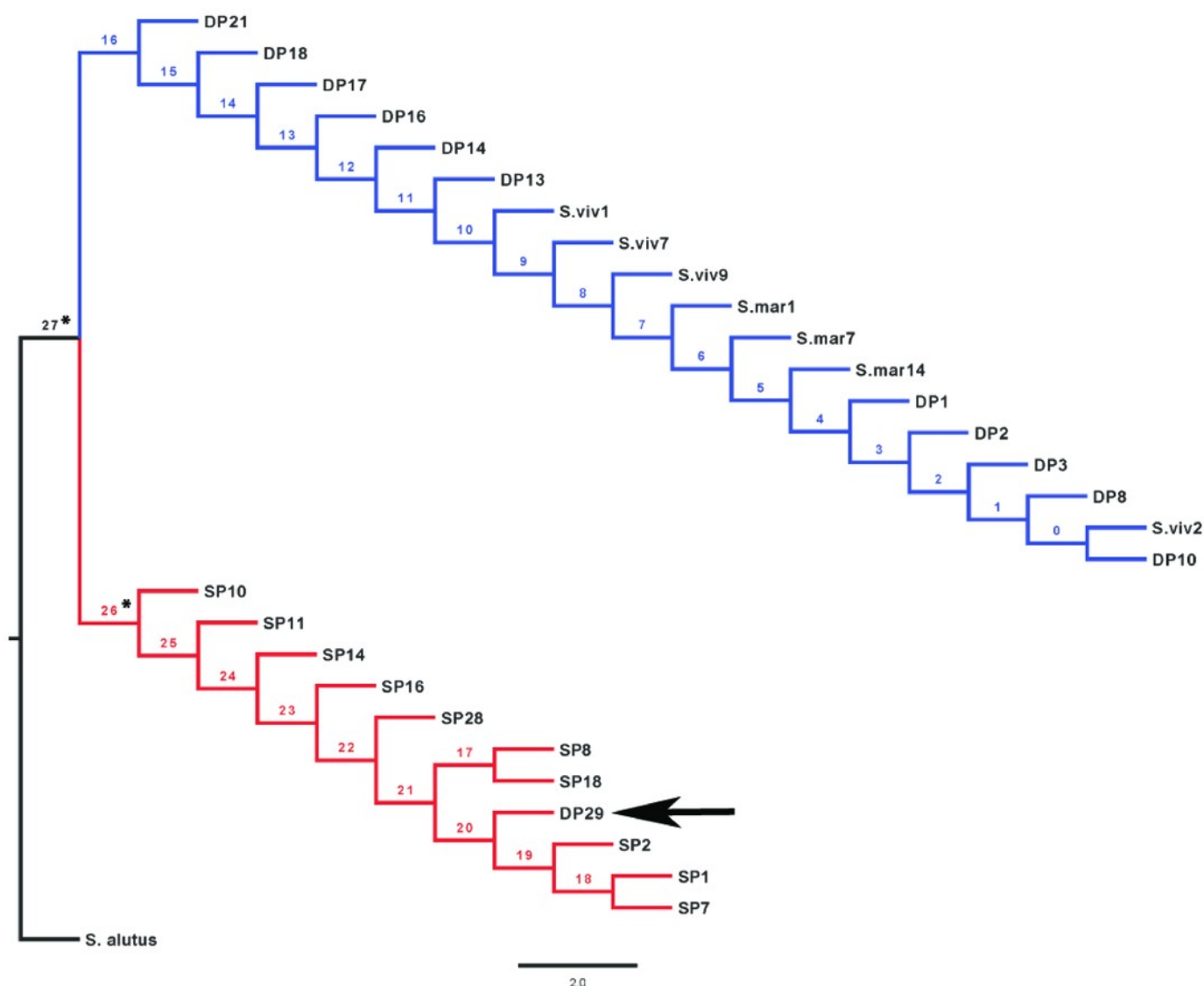


# Figure 3

Example of non-synonymous base substitution

Figure 3. Chromatograms illustrating the non-synonymous A/G mutation on the rhodopsin gene, which discriminates between “Deep-Pelagic” (a: above) and “Shallow-Pelagic” (b: below) *Sebastes mentella*.

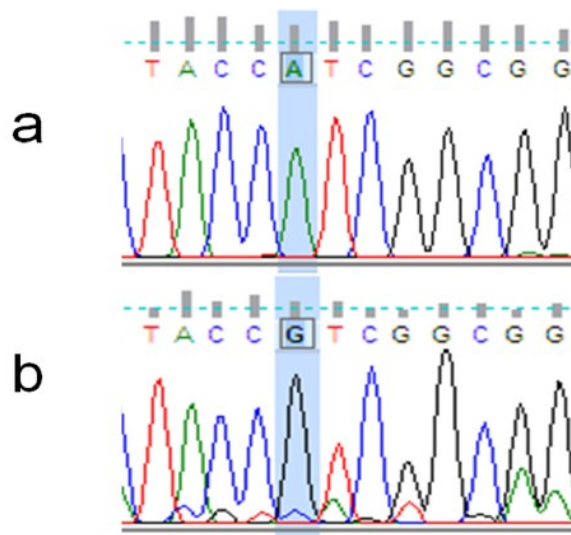


# Figure 4

## Ordination of microsatellite genotypes

Figure 4. Correspondence analysis based on microsatellite data. Each circle represent an individual, red and blue refer to the shallow-pelagic (SP) and deep-pelagic (DP) groups respectively.

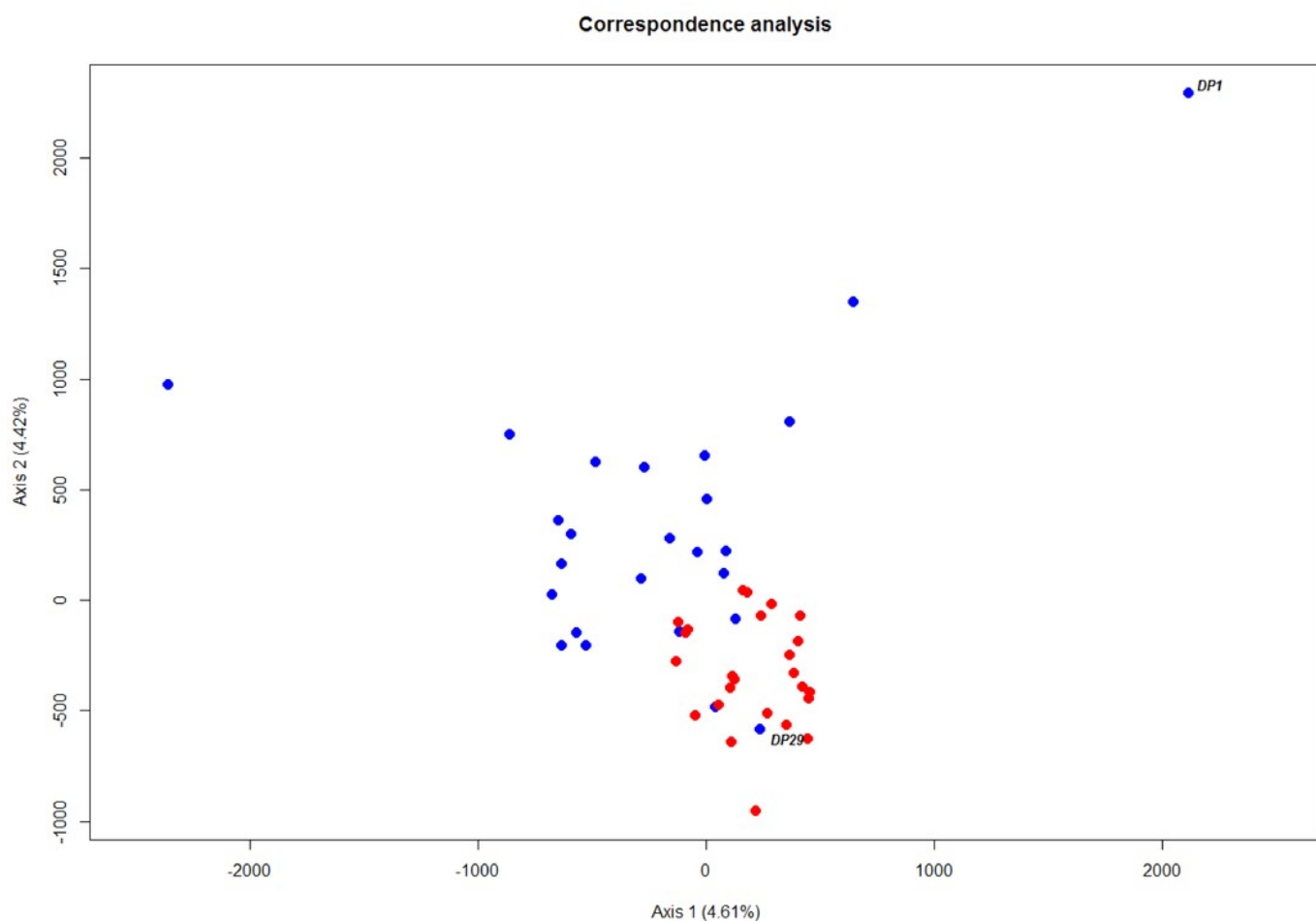




# **Table 1** (on next page)

Summary of mtDNA control region molecular

**Table 1.** Summary of mtDNA control region molecular diversity: H = unique haplotypes; n = number of individuals; S = Segregating sites; FS = Fu's FS statistic; DT = Tajima's D ; F\* = Fu and Li's F test; D\* = Fu and Li's D test. SP = Shallow Pelagic; DP = Deep Pelagic.

| Population | H/n  | S  | $\hat{h} \pm SD$ | $\hat{D} \pm SD$ | $D_T$    | $F_S$  | $F^*$    | $D^*$    |
|------------|------|----|------------------|------------------|----------|--------|----------|----------|
| (SP)       | 8/25 | 10 | 0.887±0.03       | 0.00504±0.0008   | -1.08590 | -3.806 | -2.30037 | -2.35314 |
| (DP)       | 6/25 | 8  | 0.543±0.11       | 0.00238±0.0007   | -1.77639 | -4.717 | -1.49744 | -1.08199 |

## Table 2<sub>(on next page)</sub>

Analysis of fixation/differentiation indices for mtDNA and microsatellite data between shallow-pelagic (SP) and deep-pelagic (DP) *S. mentella*.

**Table 2.** Analysis of fixation/differentiation indices for mtDNA and microsatellite data between shallow-pelagic (SP) and deep-pelagic (DP) *S. mentella*.

| Marker          | Group    | Fixation/Differentiation index | estimate | <i>p</i> |
|-----------------|----------|--------------------------------|----------|----------|
| mtDNA           | SP vs DP | $F_{ST}$                       | 0.636    | <0.001   |
|                 |          | $\Phi_{ST}$                    | 0.273    | <0.001   |
| Microsatellites | SP vs DP | $F_{ST}$                       | 0.031    | 0.001    |
|                 |          | $G'_{ST}$                      | 0.135    | 0.001    |
|                 |          | $D_{est}$                      | 0.121    | 0.001    |

# **Table 3**(on next page)

Mismatch distribution parameter estimates for mtDNA control region

**Table 3.** Mismatch distribution parameter estimates for mtDNA control region

| Population | $\tau$ | $\theta_0$ | $\theta_1$ | Mismatch Distribution   |                         |
|------------|--------|------------|------------|-------------------------|-------------------------|
|            |        |            |            | SSD $p$ -value $\pm$ SD | $r$ $p$ -value $\pm$ SD |
| (SP)       | 1.9    | 0.0000     | 99,999     | DE                      | 0.30 $\pm$ 0.21         |
|            |        |            |            | 0.007 $\pm$ 0.18        |                         |
|            |        |            |            | SE                      | 0.27 $\pm$ 0.28         |
| (DP)       | 0.1    | 0.0000     | 99,999     | DE                      | 0.00 $\pm$ 0.21         |
|            |        |            |            | 0.274 $\pm$ 0.18        | 0.67 $\pm$ 0.28         |
|            |        |            |            | SE                      | 0.004 $\pm$ 0.002       |

$\tau$  = tau;  $\theta_0$  = theta 0;  $\theta_1$  = theta 1; SSD = sum of squared deviations;  $r$  = raggedness

statistic; DE: demographic expansion, SE: spatial expansion; (SP) = Shallow pelagic; (DP) = Deep-pelagic.

# **Table 4**(on next page)

Creevey-McInerney positive selection analysis on *Sebastes* rhodopsin sequences outgrouped with *S. alutus* (GenBank: EF212407.1), G-value  $p < 0.05$  for Fisher's† and G-Test\*

**Table 4.** Creevey-McInerney positive selection analysis on *Sebastes* rhodopsin sequences outgrouped with *S. alutus* (GenBank: EF212407.1), G-value  $p < 0.05$  for Fisher's† and G-Test\*

| Branch no. | RI | RV | SI | SV | G-value |
|------------|----|----|----|----|---------|
| rhodopsin  |    |    |    |    |         |
| 0          | 0  | 2  | 0  | 0  | 0.00    |
| 1          | 0  | 2  | 0  | 0  | 0.00    |
| 2          | 0  | 2  | 0  | 0  | 0.00    |
| 3          | 0  | 5  | 0  | 0  | 0.00    |
| 4          | 0  | 5  | 0  | 0  | 0.00    |
| 5          | 0  | 5  | 0  | 0  | 0.00    |
| 6          | 0  | 5  | 0  | 0  | 0.00    |
| 7          | 0  | 5  | 0  | 0  | 0.00    |
| 8          | 0  | 5  | 0  | 0  | 0.00    |
| 9          | 0  | 5  | 0  | 0  | 0.00    |
| 10         | 0  | 5  | 0  | 0  | 0.00    |
| 11         | 0  | 8  | 0  | 0  | 0.00    |
| 12         | 0  | 8  | 0  | 0  | 0.00    |
| 13         | 0  | 8  | 0  | 0  | 0.00    |
| 14         | 0  | 8  | 0  | 0  | 0.00    |
| 15         | 0  | 8  | 0  | 0  | 0.00    |
| 16         | 0  | 11 | 1  | 0  | 2.01    |
| 17         | 0  | 0  | 1  | 0  | 0.00    |
| 18         | 0  | 9  | 0  | 0  | 0.00    |
| 19         | 0  | 11 | 0  | 0  | 0.00    |
| 20         | 0  | 12 | 0  | 0  | 0.00    |
| 21         | 0  | 12 | 0  | 0  | 2.2     |
| 22         | 0  | 12 | 1  | 0  | 2.2     |
| 23         | 0  | 12 | 1  | 0  | 2.2     |
| 24         | 0  | 12 | 1  | 0  | 2.2     |



|    |   |    |   |   |                  |
|----|---|----|---|---|------------------|
| 25 | 0 | 12 | 1 | 0 | 2.2              |
| 26 | 1 | 12 | 2 | 0 | 5.5 <sup>†</sup> |
| 27 | 8 | 24 | 5 | 1 | 6.76*            |